Available online at www.sciencedirect.com

Manufacturing Letters

Manufacturing Letters 00 (2023) 000–000

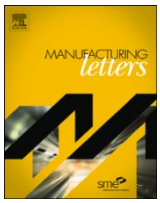

51st SME North American Manufacturing Research Conference (NAMRC 51, 2023)

FFF-based Metal and Ceramic Additive Manufacturing: Production Scale-up from a Stream of Variation Analysis Perspective

Blake Ray[a,b], Boris Oskolkov[c], Chenang Liu[c], Zacary Leblanc[d], Wenmeng Tian[a,e]*

[a] *Department of Industrial and Systems Engineering, Mississippi State University, Mississippi State, MS 39762, USA*
[b] *Department of Engineering Technology, Wallace State Community College, Hanceville, AL 35077, USA*
[c] *The School of Industrial Engineering & Management, Oklahoma State University, Stillwater, OK 74078, USA*
[d] *Department of Mechanical Engineering, Mississippi State University, Mississippi State, MS 39762, USA*
[e] *Center for Advanced Vehicular Systems, Mississippi State University, Mississippi State, MS 39762, USA*

* Corresponding author. Tel.: +1 662.325.7625; fax: +1 662.325.7618. E-mail address: tian@ise.msstate.edu

Abstract

Metal and ceramic fused filament fabrication (FFF) has been increasingly used additive manufacturing (AM) processes in the various applications including product prototyping and rapid tooling. Due to its high flexibility in both material composition and part design fabrication, metal and ceramic FFF has shown significant potential in fabricating various functional structures with specific properties of interest, such as mechanical property and thermal conductivity. Moreover, those FFF processes have also demonstrated phenomenal advantages over the other AM technologies, including its cost and energy efficiency. However, the quality control for these processes is still in its infancy, which hinders their broader adoption in more mission critical applications. Therefore, there is an urgent need in understanding the process-structure-property relationships in the metal and ceramic FFF. Both metal and ceramic FFF processes are generally composed of three major steps, i.e., materials preparation, FFF, and post-treatment. In this paper, the state-of-the-art studies on metal and ceramic FFF has been examined from a stream of variation (SoV) analysis perspective, where the variation sources introduced in each step are investigated and the metrological methods to characterize those variation are summarized. Furthermore, research opportunities and challenges for the quality control for the production scale-up of the FFF-based metal and ceramic AM are discussed.

© 2023 Society of Manufacturing Engineers (SME). Published by Elsevier Ltd. All rights reserved.
This is an open access article under the CC BY-NC-ND license (http://creativecommons.org/licenses/by-nc-nd/4.0/)
Peer-review under responsibility of the Scientific Committee of the NAMRI/SME.
Keywords: Additive manufacturing; ceramic; fused filament fabrication; geometric accuracy; metal; stream of variation

1. Introduction

Fused filament fabrication (FFF) has become one of the most widely used additive manufacturing (AM) technologies, due to its ease of use, versatility, robustness, and cost-effectiveness [1], [2]. This AM process has been applied to diversified engineering and research fields, including biomedical studies with micro-components [3], printed electrical conductors [4], antimicrobial toy manufacturing [5], development of surgical implants [6], composites research [7], [8], aerospace component design [9], as well as general educational purposes [10]. With such a diverse array of fields and applications, the FFF process has been extended from printing using pure polymer materials to various other materials, such as metal and ceramic, using the polymer as binder material to facilitate the printing process. Metal and ceramic material filaments are formed by combining more than one types of materials, each with their own physical and chemical properties, and extruding into a filament form. The diversified possible combinations of those materials facilitate the metal and ceramic FFF builds to achieve certain customized properties that the pure materials could not achieve on their own. For example, the highly-filled polymers containing various metal or ceramic micro-powders demonstrate

2213-8463 © 2023 Society of Manufacturing Engineers (SME). Published by Elsevier Ltd. All rights reserved.
This is an open access article under the CC BY-NC-ND license (http://creativecommons.org/licenses/by-nc-nd/4.0/)
Peer-review under responsibility of the Scientific Committee of the NAMRI/SME.

significantly more favorable properties (e.g., thermal conductivity [11], mechanical properties [12], [13]) when compared with the pure polymer FFF builds.

Regarding metal and ceramic material FFF's applications, the ability to produce complex geometries enables engineers to streamline the process between design and finished product. When compared with other AM processes in fabricating similar materials, FFF demonstrates lower equipment cost [14], higher build rates [13], enhanced flexibility in material composition [15], as well as lower energy consumption [16]. Given all the significant advantages of FFF, it has received growing attention from the manufacturing research community in the past years, as illustrated in Figure 1. The data in the figure were collected from google scholar search using keywords of "FFF" and "ceramic"/ "metal" within specific years.

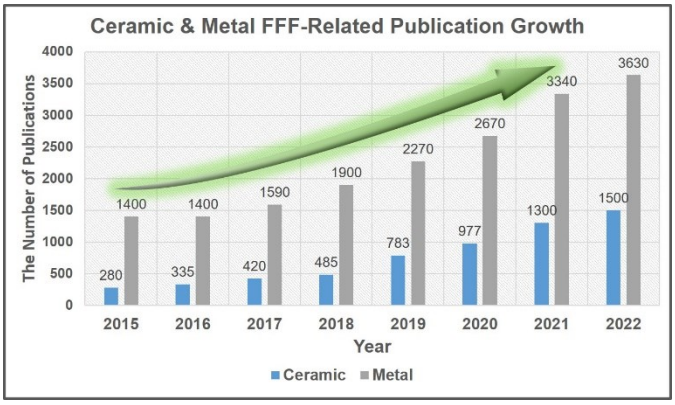

Figure 1: Ceramic & Metal FFF-related Research Growth from Year 2015 to 2022

Although a growing number of studies published, the research in process modeling, monitoring, and control for metal and ceramic FFF is still in its infancy. Moreover, the high process complexity and flexibility in material composition make the modeling and quality control an unprecedently challenging task. Therefore, there is an urgent need in systematically reviewing and characterizing the stream of variations in the metal and ceramic FFF process. The outcome of interests of the process include geometric dimensioning and tolerancing (GD&T) aspects (e.g., dimensional variations and surface roughness) and mechanical properties (e.g., tensile strength and fatigue behaviour).

As illustrated in Figure 3, the metal and ceramic FFF process can be regarded as a multi-stage process, which involves three stages: ***1) material preparation*** involves the fabrication of composite filament which incorporates mixing and extruding the composite material to the filament form [17]; ***2) FFF*** is referred to as the material extrusion 3D printing process using the composite filament to fabricate the designed geometry in a layer-by-layer manner; and ***3) post-treatment*** includes the necessary debinding operations to remove the binding agent in the composite to obtain the part composed of the pure material of interests [18], as well as sintering the printed part for improved density and mechanical strengths. Within the three stages, the outcomes of the previous stage are critical input of the consecutive stage, which aligns well with the context of stream of variation (SoV) analysis [19].

Therefore, this paper aims to highlight the state-of-the-art studies on metal and ceramic FFF from an SoV analysis perspective, where a complex multi-stage process can be analysed by elucidating all the variation sources and their interactions in the process. The SoV analysis enables the comprehensive characterization of the metal and ceramic FFF process in a unified model-based framework, leading to statistical quantification and reduction of the final product variation [19]. The multi-stage nature and highly flexible material composition makes it complicated to characterize and control the variation in the FFF process, leading to significant challenges in the quality control of the final parts.

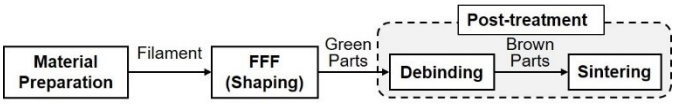

Figure 3: Major steps of metal and ceramic FFF

The reminder of this paper is organized as follows. Section 2 reviews and analyses the state-of-the-art metal and ceramic FFF studies by focusing on the variation introduced at each major stage. Subsequently, section 3 highlights the remaining challenges and opportunities in the production scale-up of metal and ceramic FFF, and section 4 summarizes the conclusion of this review paper.

2. Stream of variation analysis for metal and ceramic FFF

In this section, the SoV in metal and ceramic FFF is analyzed by highlighting the state-of-the-art studies related to each step, i.e., materials preparation, FFF (shaping), and post-treatment. More specifically, the major variation sources and their

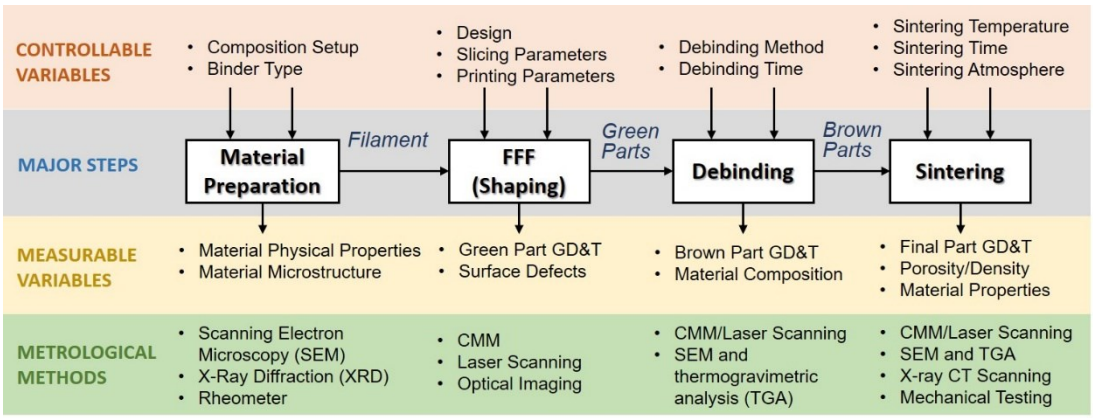

Figure 2: Overview of the SoV Analysis in Metal and Ceramic FFF

corresponding metrological methods that can be used for characterization are summarized for each fabrication step. An overview of the SoV analysis is illustrated in Figure 3.

2.1. Material preparation

The feasibility of different metal and ceramic materials for FFF has been extensively explored in recent studies. The investigated materials as well as the quality outcomes have been briefly summarized in Table 1. In general, these materials can be divided into three groups: alloys, pure metals, and ceramics. Notably, the investigation on alloys has attracted more attention [20], [21]. In addition, fiber-reinforced polymers (FRP) has also been well studied in the literature [22], and the material preparation information has been summarized in Appendix I.

Table 1: Summary of metal and ceramic materials fabricated using FFF (Nd: Nozzle diameter, Pt: Printing temperature)

Composition	Binder	Material property/potential applications	Machine setup	Notable quality outcomes
Alloys				
Titanium (Ti–6Al–4 V) [15], [23], [24]	APP, CW, DBP, EVA, PW, PVA, PP-PE, PIB, SA	• Corrosion resistance • Stress-corrosion • High strength • Good ductility and strength • Bioinert	• Nd: 0.4 mm • Pt: 170–210, or 240 °C	• Isotropic mechanical properties • Low porosity
Stainless Steel (17–4PH) [25]–[27]	PW, PE, Polyolefin, SA, TPE, POM, PP	• Acid- and corrosion resistant prototypes manufacturing • Unique or series production parts in plant engineering, automotive industry, medical technology, jewelry	• Nd: 0.3–0.6 mm • Pt: 175, or 210–250 °C	• Cost-effective with similar quality • Anisotropic shrinkage and mechanical properties still the problem for relatively big parts
Stainless Steel (316L) [28]–[32]	DOP, DBP, LDPE, HDPE, POM, PW, SA, TPE, SEBS, PP, ZnO	• Corrosion resistance, ductility, and biocompatibility, with promising structural applications and biomedical uses. • Low strength and wear resistance	• Nd: 0.2–0.8 mm • Pt: 170–240, or 270–290 °C	• Cost-effective • Binder system significantly influence part's properties • Nozzle size is important
Tungsten carbide/cobalt (WC-10Co) [33], [34]	TPE	• Hard metal • Wear-resistant parts • Cutting tools • Mining part for excavation	• Nd: 0.3 mm • Pt: 190 °C	• Low residual stress • Uniform microstructure • Low powder requirements • No raw material loss
Titanium carbo-nitride Ti (C, N)	nNi, PLA, PEG, PEI	• Electronics' packaging • Cutting inserts • Noncutting shaping tools	• Nd: 0.3 mm • Pt: 155 °C	• Excellent sintering behavior
Neodymium magnet $Nd_2Fe_{14}B$ [35]	PA 11	• Strong magnetic material	• Nd: 0.3 mm • Pt: 200–245 °C	• Cost-effective • Low dimension accuracy
Bronze (CuSn) [36]	PLA	• Bearing parts	• Pt: 215 °C	• Cost-effective • Good mechanical properties
Pure metal				
Copper (Cu) [37]–[39]	ABS, TPE, PP, PO, PLA, PW	• Lightweight • Thermally and electrically conductive	• Nd: 0.3 mm • Pt:120, or 160–180 °C	• Cost-effective
Iron (Fe) [37], [40]–[42]	Nylon, polyolefin-elastomer	• Motor parts • Bone tissue engineering applications	• Nd: 0.3 mm • Pt: 155 °C	• Thermal conductivity depends on metal filling • Hydrophilic wetting behavior • Cytocompatibility • Surface post-processing needed
Ceramics				
Titania (TiO_2) [43]	PLA, PA, PP, PCL, PEEK, PMMA	• Antimicrobial applications, food packaging	• Nd: 0.4 mm • Pt: 210 °C	• Low porosity • Good mechanical properties
Zirconia (ZrO_2) [44], [45]	LDPE, PW	• Resistance to chemicals and corrosion • Dental frameworks • Insulating rings	• Nd: 0.6, 2.8 mm • Pt: 160 °C	• Low porosity
Alumina (Al_2O_3) [46]	Polyolefin, PLA	• Electrically and thermally insulating, high hardness, resistance to abrasion • Resistance to chemicals and corrosion • Wear resistance	• Pt: 150 °C	• Low porosity • Comparable to conventional manufacturing methods
Molybdenum disilicide ($MoSi_2$) [45]	LDPE	• Heating elements	• Nd: 0.6 mm • Pt: 160 °C	• Promising to print reliable and functional parts
Barium ferrite ($BaFe_{12}O_{19}$) [47]	ABS	• Ferrimagnetic parts: filters, magnets	• Nd: 0.4 mm • Pt: 230 °C	• Demand several specific adjustments like enhanced printer, external alignment field. • Process optimization needed.
Strontium ferrite ($SrFe_{12}O_{19}$) [48]	PA 12		• Nd: 0.3 mm • Pt: 260 °C	
Chalcogenide glass ($As_{40}S_{60}$) [49]	LDPE, PP	• Lenses • Light guides	• Nd: 0.4 mm • Pt: 330 °C	• No advantages compared to classic manufacturing methods yet
Yttria stabilized zirconia (YSZ) [50]	Pluronic F-127	• Dental frameworks • Refractory • Implants for surgery	• Nd: 0.58 mm • Pt: 220 °C	• Notable dependence between part properties and machine setup

To incorporate metal or ceramic materials in FFF, it is important to use an appropriate binder composition as well as printing under optimized printing conditions, as mentioned in [32]. The FFF printed alloy parts are more cost effective (especially for one-piece production) [25], [28] than other 3D printing processes, such as powder bed fusion and directed energy deposition. With the optimized material composition and machine setup, FFF can also achieve comparable quality. For the research on pure metal FFF, a lot of existing studies are focused on copper [39] and stainless steel [51], which can be used as thermal conductors and load-bearing structures, respectively. More studies for the other potential of metals in FFF are still urgently needed [21].

Ceramic FFF composites have shown a great demand from the manufacturing community [45] due to their unique properties, specifically, their resistance to different chemical, biological and thermal conditions. These properties give great opportunities in many areas, such as medical applications [52], [53]. Overall, ceramic FFF is promising and has the potential to reduce the manufacturing costs. Regarding the quality concerns, the recent research has achieved significant results in reducing the main quality issues of FFF printed ceramics, i.e., the porosity [43]. In addition, it is still worth paying attention to the glass composites. As shown in [54], glass is not very suitable for 3D printing, it might be challenging to observe notable development progress in glass composites for FFF.

The ***major variation sources*** of the material preparation step include material composition and the properties after composition. These variations are resulted of composition setup and binder selection. To quantify these variations, the metrological devices for material characterization, such as the scanning electron microscopy (SEM) and X-Ray Diffraction (XRD), can be used [55]. Furthermore, the rheological behaviour of the filament material is of significant importance in the material preparation as well as the subsequent FFF printing process. The rheological measurements can be captured by the rheometer [56], [57].

2.2. FFF (shaping)

The FFF step involves the part design, slicing, and 3D printing to obtain the green parts. In this subsection, the controllable inputs in the FFF step are summarized, and the variation introduced in this step is highlighted.

The ***design*** artifacts are generated to test the specific part outcome of interests. To test the material property obtained from the FFF, standard testing coupons, such as various dog-bone designs, can be fabricated for tensile testing [25], [58]. To examine the porosity, compressive strength, shrinkage, and infill adhesion of the printed material, basic rectangular prism is generally used [59], [60]. Moreover, to test the thermal conductivity of the printed part, cylindrical shaped specimen can be fabricated [11]. More recently, researchers have started focusing on part designs that are more complicated than the standard testing coupons. For example, to study the surface roughness of the resulting surface, parallelepiped shaped specimen can be fabricated to examine the surfaces characterized for different building orientations [61]. In addition, to characterize the specific deformation patterns in the overhang structures, various overhang structures with different build angles can be fabricated [51].

The ***slicing and printing process*** of the green parts involves various slicing and printing parameters, which are the major parameters used to optimize the FFF. Previous studies have shown that the slicing settings (including nozzle diameter, layer thickness, raster pattern, infill percentage, and building orientation) as well as the printing parameters (e.g., printing speed and temperature) significantly affect both mechanical performance and geometric accuracy of metal and ceramic FFF parts. Caminero *et al.* [28] demonstrated the impacts of extruder nozzle size on stainless steel printed with a

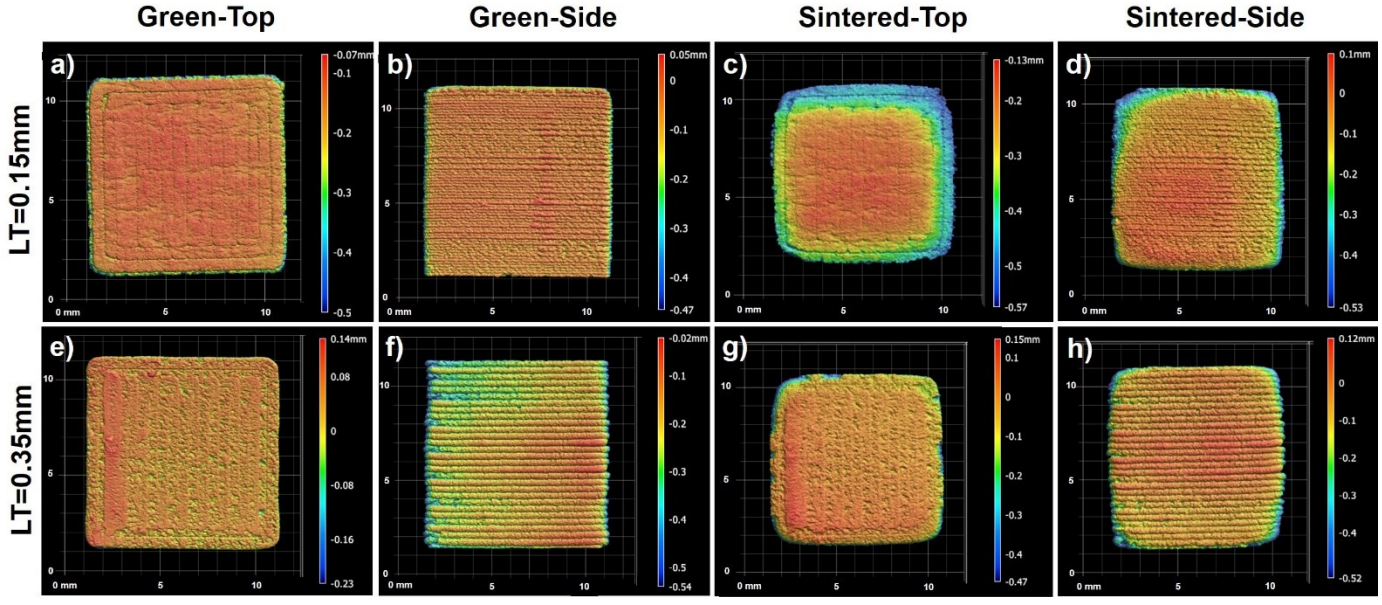

Figure 4: Surface variation of the green and sintered parts based on different slicing parameters: each row contains the scans of the top/side surface of the green/sintered part. The surface scan data were collected using the wide-area 3D measurement system by Keyence Corporation. (LT: layer thickness)

polyformaldehyde-based binder system and found that increasing the nozzle diameter of the extruder resulted in a decrease in porosity, which in turn, produced stronger mechanical properties of the printed parts. On the other hand, variations in the geometry, as well as surface roughness, both decreased as a result in lowering the nozzle diameter. In relation to nozzle diameter, it is also important to focus on filament flow rate. Godec *et al.* [62] tested the effects of extrusion temperature, layer thickness, and flow rate on the tensile strength of 3D printed 17-4PH stainless steel samples with a multicomponent binder. The experiments showed that, among all three of these printing parameters, tensile strength of the steel was most affected by the flow rate multiplier. Namely, the increased flow rate creates denser parts. In this case, the strands of material are able to intersect and attach. This causes a reduction in the number of cavities between individual strands of material in the printed parts.

Another slicing setting that adds more material to the parts is infill density, which has also been shown to increase part mechanical properties. Ait-Mansour *et al.* showed that increasing the infill levels will increase the compressive strength of 3D printed 316L stainless steel [63]. Furthermore, both experiments evaluated the effects of build orientation on mechanical performance. It has been proven that build orientation can have a substantial impact on the mechanical performance of parts printed using the FFF process. With 3D printed parts, pore structure is highly dependent on the layer direction on the build platform. Therefore, build orientation is vital to the mechanical properties, especially tensile strength, of the completed parts [13], Parts printed in on-edge and flat build orientations have been shown to maintain low average porosity levels when compared to the upright orientation. For this reason, parts can be printed near full density using the FFF process [28].

The ***major variation sources*** of the FFF step are the green part GD&T features, including the geometric and dimensioning deviation and surface roughness. These variations are resulted from the slicing and printing process parameter selection as well as their resulting process uncertainty. To quantify the geometric and dimensioning deviations both contact based coordinate measuring machines (CMM) and noncontact-based laser scanning can be used to generate a point cloud to fully capture the geometry of the fabricated green parts [51], [64], [65]. To characterize the surface roughness, both contact-based profilometers and non-contact based scanning or imaging systems can be used [61], [66], [67]. For example, the two 10mm Inconel cubicle parts were printed using different layer thickness (i.e., 0.15mm and 0.35mm), and the surfaces of the green parts and brown parts were characterized, as illustrated in Figure 4.

2.3. Post-treatment

As the polymer in the filament serves as the binding agent for the major material constitute (e.g., metal or ceramic powders), the green parts need to go through the post-treatment procedure to remove the binding agent and increase the material density, leading to the final product with 100% major material constitute. The post-treatment of the green parts usually involves debinding and sintering. Debinding is used to remove the polymeric binder in the green parts, resulting in the "brown" parts. On the other hand, during the sintering process, the brown parts are heated to temperatures that are below the melting temperature of the major constituent in metal for a pre-determined period of time. These post-treatment procedures are critical to generate the desired dense structure.

There are three main ***debinding*** methods, i.e., thermal, solvent, and catalytic debinding [68], [69]. Thermal debinding heats the green parts in a furnace, and the debinding temperature is determined by the thermogravimetric analysis (TGA) of the polymer binder. The temperature and heating rates are also determined by geometry of the part and the material, where a higher heating rate is usually favorable, unless the accelerated heating generates cracks in the resultant brown parts. Solvent debinding uses a solvent to remove the binders in the green parts, and the required treatment time is highly dependent on the shape and size of the cross-sectional area of the part. It is worth noting that the required treatment time for solvent debinding is exponentially increased with the wall thickness [31]. Catalytic debinding is offered by the filament of BASF SE. This patented technology facilitates a faster binder removal rate than the traditional thermal and solvent debinding [70]. It is worth noting that the latter two techniques will not remove all the polymetric binders in the green parts. On the contrary, some polymer material is needed to remain in the green-brown parts, serving as the backbone material to retain the part geometry. To fully remove all the polymetric binder material, these parts need to go through a pre-sintering routine, where the temperature usually ranges between 200 °C and 600 °C [71]. During the ***sintering*** process, the brown parts are heated to temperatures below the melting point of the material for a specified holding time. The duration of the holding period is primarily determined by the part size. During the sintering process, the internal atmosphere of the furnace needs to be strictly controlled, where different types of gas are needed for sintering different material. Detailed summaries of the debinding and sintering process parameters for different materials have been provided in a few recent literature papers [20], [69].

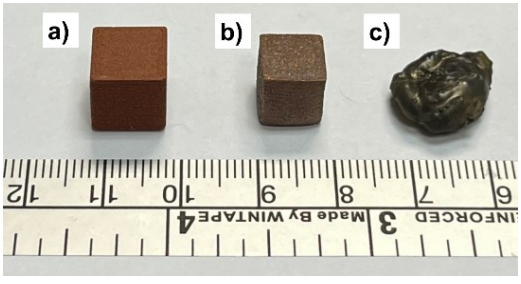

Figure 5: Sample specimen before and after the post-treatment procedure: a) A green part fabricated using the copper filament by Virtual Foundry; b) A brown part after post-treatment with significant shrinkage and slight deformation; and c) A brown part after failed post-treatment with excessive heating and oxidization.

The ***major resulting variation*** of the post-treatment step are the final part GD&T features, including the geometric and dimensioning deviation and surface roughness. These

variations can be attributed to all the controllable variables and process uncertainty in all the three major steps. Basically, all the process variation can in the previous steps can be propagated to the final part GD&T and material properties. In addition, the post-treatment step itself leads to new variation in part deformation and shrinkage, as illustrated in Figure 5.

3. Remaining challenges and opportunities in scale-up of metal and ceramic FFF

Based on the SoV analysis conducted in section 2, a few research challenges and opportunities have been identified in scaling up the production of metal and ceramic FFF, including online sensing and data acquisition, as well as process modeling and control.

3.1. Online sensing and data acquisition for quality management

Due to the significant quality concerns reported from the recent studies [20], [72], to achieve effective online sensing and data acquisition, which is crucial for process quality management [73], is also an important research direction to be further explored. Recently, online sensing and data acquisition have demonstrated great success and potential in the conventional FFF, which can make great contributions to monitoring the process quality and help with the variation reduction [1], [74], [75]. However, due to the uniqueness in the metal and ceramic FFF, such as the complex material composition and different requirements of machine/process setup, there are still several remaining key gaps, which can be summarized into two main aspects, as discussed below.

Appropriate sensor selection for the printing process: The recent studies for the conventional FFF have explored a large variety of sensors and investigated their effectiveness, for example, the vibration sensors [74], [76], thermal/infrared sensors [77], [78], acoustic sensors [79], [80], optical devices [81], [82], 3D scanner [67], etc. Due to the same material extrusion nature for the metal and ceramic FFF, these sensors can still provide valuable information. For example, the thermal sensors, as temperature still plays a significant role in the printing process [74]. However, due to the higher complexity of materials and more critical factors in the process setup, sensor selection still needs to be further investigated and validated for enabling comprehensive online process data acquisition in metal and ceramic FFF, so that better process quality management can be achieved. First, the expected sensing capability may be different. For example, since the nozzle diameter is usually much larger than the conventional FFF, the width of printing path will also be larger. Thus, to collect the real-time printing surface data via optical devices (e.g., digital microscopes [83], [84]), larger field of view (FoV) will be desired. Similarly, if considering the vibration or acoustic sensors, the appropriate sensing capability should also be investigated. Second, more types of sensors may also be explored, in order to cover the sensing for more process variables. For example, it would be helpful if the data for the density of composition after deposition as well as the re-melting (for binder) or oxidizing (if metal) effects can be obtained through appropriate sensors.

Suitable in-process sensing strategy for sintering: As discussed before, different from the conventional pure material FFF, sintering is usually required to complete the part fabrication in the metal and ceramic FFF [69]. Thus, how to perform suitable sensing for the sintering process should also be a critical aspect in online data acquisition. As sintering has been applied to various additive manufacturing processes, such as the selective laser sintering (SLS) [85], [86], the sensing strategy in these processes may be considered in the sintering for metal and ceramic FFF parts. For example, the infrared camera may be considered to obtain the thermal distribution of the part during sintering [87], which may help to better understand the part properties and defect formation introduced by sintering. However, the installation and cost effectiveness still need to be investigated.

3.2. Process modeling and control

To further understand the process and improve the quality of fabricated parts, with the assistance of quality characterization and online sensing, effective process modeling and control are also critical needed. However, the related research is still limited. According to the existing studies in AM, this section will discuss three potential research directions, and their inter-connections are also illustrated in Figure 6.

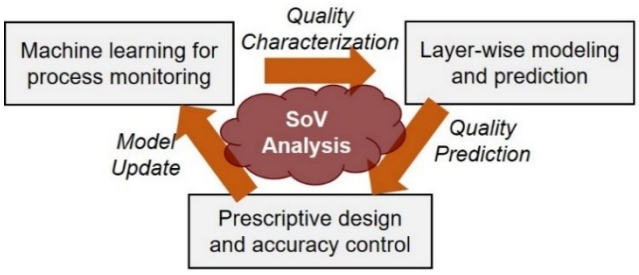

Figure 6: The inter-connections of the three potential research directions for process modelling and control in metal and ceramic FFF.

Data fusion and pattern recognition for process monitoring and control: To achieve effective process monitoring, it is beneficial if all the data related to the process quality can be utilized, in which data fusion and machine learning can contribute. For example, data fusion could extract the critical quality information from the high dimensional multi-source data, and then machine learning can also help to understand the variation from the extracted information for process monitoring [75], [88]–[90]. As shown in Figure 6, the extracted quality characteristics can also be the input for layer-wise modeling and prediction. Moreover, this outcome can also further facilitate the implementation of online close-loop quality control, by leveraging appropriate the decision-making techniques, e.g., PID control [91] and reinforcement learning [92], which has been successfully implemented in the conventional pure material FFF.

Layer-wise modeling and prediction: Similar to all other AM processes, it is also important for metal and ceramic FFF to implement layer-wise modeling and prediction, which can help to better understand the process dynamics and thus enable effective process optimization. As the statistical methods [93],

[94] and machine learning models [95], [96] have demonstrated great potential in layer-wise modeling and prediction of various AM processes, it also provides a promising direction to achieve effective modeling for the process variation in metal and ceramic FFF.

Prescriptive design and accuracy control: To reduce the final part's deviation from the nominal design, developing prescriptive design and accuracy control approach for the metal and ceramic FFF would be very helpful. Similar research has been conducted in other popular AM processes (e.g., SLA) and demonstrated promising performance [97]–[99]. In the metal and ceramic FFF, one major uniqueness is the sintering process, which may lead to significant geometric deformation and structural porosity. Thus, a computational model that can evaluate and predict such variation and suggest the design compensation is greatly needed.

4. Conclusions

This work provides an overview for the stream of variation analysis in the metal and ceramic FFF, through the review of existing studies and our preliminary printing experiments. According to the review and analysis, it can be observed that the metal and ceramic FFF can provide a cost-effective manufacturing solution with product quality potentially comparable to more expensive AM solutions. However, due to the significant process variation induced in all the three manufacturing stages (i.e., the material preparation, FFF, and post-treatment), it still requires dedicated research efforts to fully characterize the variation propagation in this multi-stage process to accelerate the adoption of the metal and ceramic FFF. Opportunities and challenges with quality control for scale-up of the metal and ceramic FFF remains, but also lends itself to improvements through better understanding of process variations.

With the identified key sources of variations in this work, the remaining gaps and future research opportunities to further reduce the process variation and better manage the product quality are also identified, including but not limited to: 1) quality characterization; 2) online sensing and data acquisition; as well as 3) process modeling and control. The extensive research progress of these three fields in other popular AM processes also provides strong confidence and inspiration to its potential of success in the future.

Appendix I: FRP materials fabricated using FFF

Composition	Machine setup	Notable quality outcomes
Carbon fiber powder [100]	• Nd: 0.35 mm • Pt: 230 °C	• 100 μm fiber length specimen showed higher ductility and toughness with respect to 150 μm.
Short carbon fiber [101]	• Nd: 0.5 mm • Pt: 205 °C	• Higher tensile strength and modulus compared with the conventional compression molded composites
Short glass fiber [102]	• Pt: 200 °C	• Strength of ABS was improved significantly at the expense of handleability and poor flexibility.
Carbon fiber-reinforced (CFR) [103], [104]	• Nd: 0.5 mm • Pt: 215 or 230 °C	• Carbon fiber greatly improve mechanical characteristics • Printing speed and nozzle temperature should match. • Higher modulus was obtained for higher infill density. • CFR-PLA was found to be the strongest material.
Carbon nanotube-reinforced (CNT) [103], [105], [106]	• Nd: 0.2, 0.5, 0.8 mm • Pt: 230 or 365 °C	• CNT does not affect the mechanical properties of the PEEK parts

Acknowledgements

This work is partially supported by National Science Foundation CMMI-2046515. The authors would like to thank Dr. Matthew Priddy and his group for their support in the data collection for generating Figure 4 in this manuscript. In addition, the authors would like to thank the three anonymous reviewers for their valuable comments and suggestions.

References

[1] Y. Fu, A. Downey, L. Yuan, A. Pratt, and Y. Balogun, "In situ monitoring for fused filament fabrication process: A review," *Addit. Manuf.*, vol. 38, no. July 2020, p. 101749, 2021, doi: 10.1016/j.addma.2020.101749.

[2] A. Al Rashid and M. Koç, "Fused filament fabrication process: a review of numerical simulation techniques," *Polymers (Basel).*, vol. 13, no. 20, p. 3534, 2021.

[3] D. Pranzo, P. Larizza, D. Filippini, and G. Percoco, "Extrusion-based 3D printing of microfluidic devices for chemical and biomedical applications: A topical review," *Micromachines*, vol. 9, no. 8, p. 374, 2018.

[4] T. Barši Palmić, J. Slavič, and M. Boltežar, "Process Parameters for FFF 3D-Printed Conductors for Applications in Sensors," *Sensors*, vol. 20, no. 16. 2020. doi: 10.3390/s20164542.

[5] M. A. León-Cabezas, A. Martínez-García, and F. J. Varela-Gandía, "Innovative functionalized monofilaments for 3D printing using fused deposition modeling for the toy industry," *Procedia Manuf.*, vol. 13, pp. 738–745, 2017, doi: https://doi.org/10.1016/j.promfg.2017.09.130.

[6] P. Honigmann, N. Sharma, B. Okolo, U. Popp, B. Msallem, and F. M. Thieringer, "Patient-specific surgical implants made of 3D printed PEEK: material, technology, and scope of surgical application," *Biomed Res. Int.*, vol. 2018, 2018.

[7] X. Wang, M. Jiang, Z. Zhou, J. Gou, and D. Hui, "3D printing of polymer matrix composites: A review and prospective," *Compos. Part B Eng.*, vol. 110, pp. 442–458, 2017, doi: 10.1016/j.compositesb.2016.11.034.

[8] A. D. Valino, J. R. C. Dizon, A. H. Espera, Q. Chen, J. Messman, and R. C. Advincula, "Advances in 3D printing of thermoplastic polymer composites and nanocomposites," *Prog. Polym. Sci.*, vol. 98, p. 101162, 2019, doi: https://doi.org/10.1016/j.progpolymsci.2019.101162.

[9] M. Kalender, S. E. Kılıç, S. Ersoy, Y. Bozkurt, and S. Salman, "Additive Manufacturing and 3D Printer Technology in Aerospace Industry," in *2019 9th International Conference on Recent Advances in Space Technologies (RAST)*, 2019, pp. 689–694. doi: 10.1109/RAST.2019.8767881.

[10] B. Shaqour *et al.*, "Gaining a better understanding of the extrusion

process in fused filament fabrication 3D printing: a review," *Int. J. Adv. Manuf. Technol.*, vol. 114, May 2021, doi: 10.1007/s00170-021-06918-6.

[11] N. D. Ebrahimi and Y. S. Ju, "Thermal conductivity of sintered copper samples prepared using 3D printing-compatible polymer composite filaments," *Addit. Manuf.*, vol. 24, pp. 479–485, 2018.

[12] M. Sadaf, M. Bragaglia, and F. Nanni, "A simple route for additive manufacturing of 316L stainless steel via Fused Filament Fabrication," *J. Manuf. Process.*, vol. 67, pp. 141–150, 2021.

[13] J. Damon, S. Dietrich, S. Gorantla, U. Popp, B. Okolo, and V. Schulze, "Process porosity and mechanical performance of fused filament fabricated 316L stainless steel," *Rapid Prototyp. J.*, vol. 25, no. 7, pp. 1319–1327, 2019.

[14] N. Tuncer and A. Bose, "Solid-state metal additive manufacturing: a review," *Jom*, vol. 72, no. 9, pp. 3090–3111, 2020.

[15] P. Singh, V. K. Balla, A. Tofangchi, S. V Atre, and K. H. Kate, "Printability studies of Ti-6Al-4V by metal fused filament fabrication (MF3)," *Int. J. Refract. Met. Hard Mater.*, vol. 91, p. 105249, 2020.

[16] S. Roshchupkin, A. Kolesov, A. Tarakhovskiy, and I. Tishchenko, "A brief review of main ideas of metal fused filament fabrication," *Mater. Today Proc.*, vol. 38, pp. 2063–2067, 2021.

[17] F. Calignano, M. Lorusso, I. Roppolo, and P. Minetola, "Investigation of the Mechanical Properties of a Carbon Fibre-Reinforced Nylon Filament for 3D Printing," *Machines*, vol. 8, no. 3. 2020. doi: 10.3390/machines8030052.

[18] I. Blanco, "The use of composite materials in 3D printing," *J. Compos. Sci.*, vol. 4, no. 2, p. 42, 2020.

[19] J. Shi, *Stream of variation modeling and analysis for multistage manufacturing processes*. CRC press, 2006.

[20] C. Suwanpreecha and A. Manonukul, "A review on material extrusion additive manufacturing of metal and how it compares with metal injection moulding," *Metals (Basel).*, vol. 12, no. 3, p. 429, 2022.

[21] A. I. Nurhudan, S. Supriadi, Y. Whulanza, and A. S. Saragih, "Additive manufacturing of metallic based on extrusion process: A review," *J. Manuf. Process.*, vol. 66, pp. 228–237, 2021.

[22] S. Pervaiz, T. A. Qureshi, G. Kashwani, and S. Kannan, "3D printing of fiber-reinforced plastic composites using fused deposition modeling: A status review," *Materials (Basel).*, vol. 14, no. 16, p. 4520, 2021.

[23] Y. Zhang, S. Bai, M. Riede, E. Garratt, and A. Roch, "A comprehensive study on fused filament fabrication of Ti-6Al-4V structures," *Addit. Manuf.*, vol. 34, p. 101256, 2020, doi: https://doi.org/10.1016/j.addma.2020.101256.

[24] C. Gloeckle, T. Konkol, O. Jacobs, W. Limberg, T. Ebel, and U. A. Handge, "Processing of Highly Filled Polymer–Metal Feedstocks for Fused Filament Fabrication and the Production of Metallic Implants," *Materials*, vol. 13, no. 19. 2020. doi: 10.3390/ma13194413.

[25] C. Tosto, J. Tirillò, F. Sarasini, and G. Cicala, "Hybrid Metal/Polymer Filaments for Fused Filament Fabrication (FFF) to Print Metal Parts," *Applied Sciences*, vol. 11, no. 4. 2021. doi: 10.3390/app11041444.

[26] J. Gonzalez-Gutierrez, F. Arbeiter, T. Schlauf, C. Kukla, and C. Holzer, "Tensile properties of sintered 17-4PH stainless steel fabricated by material extrusion additive manufacturing," *Mater. Lett.*, vol. 248, pp. 165–168, 2019, doi: https://doi.org/10.1016/j.matlet.2019.04.024.

[27] Y. Abe *et al.*, "Effect of Layer Directions on Internal Structures and Tensile Properties of 17-4PH Stainless Steel Parts Fabricated by Fused Deposition of Metals," *Materials*, vol. 14, no. 2. 2021. doi: 10.3390/ma14020243.

[28] M. Á. Caminero, A. R. Gutiérrez, J. M. Chacón, E. García-Plaza, and P. J. Núñez, "Effects of fused filament fabrication parameters on the manufacturing of 316L stainless-steel components: geometric and mechanical properties," *Rapid Prototyp. J.*, no. ahead-of-print, 2022.

[29] X. Kan, D. Yang, Z. Zhao, and J. Sun, "316L FFF binder development and debinding optimization," *Mater. Res. Express*, vol. 8, no. 11, p. 116515, 2021.

[30] B. Liu, Y. Wang, Z. Lin, and T. Zhang, "Creating metal parts by Fused Deposition Modeling and Sintering," *Mater. Lett.*, vol. 263, p. 127252, 2020, doi: https://doi.org/10.1016/j.matlet.2019.127252.

[31] Y. Thompson, J. Gonzalez-Gutierrez, C. Kukla, and P. Felfer, "Fused filament fabrication, debinding and sintering as a low cost additive manufacturing method of 316L stainless steel," *Addit. Manuf.*, vol. 30, p. 100861, 2019, doi: https://doi.org/10.1016/j.addma.2019.100861.

[32] D. Jiang, F. Ning, and Y. Wang, "Additive manufacturing of biodegradable iron-based particle reinforced polylactic acid composite scaffolds for tissue engineering," *J. Mater. Process. Technol.*, vol. 289, p. 116952, 2021, doi: https://doi.org/10.1016/j.jmatprotec.2020.116952.

[33] C. Berger, J. Abel, J. Pötschke, and T. Moritz, "Properties of additive manufactured hardmetal components produced by fused filament fabrication (FFF)," in *Proceedings of Euro PM 2018 Congress and Exhibition*, 2018.

[34] W. Lengauer *et al.*, "Fabrication and properties of extrusion-based 3D-printed hardmetal and cermet components," *Int. J. Refract. Met. Hard Mater.*, vol. 82, pp. 141–149, 2019, doi: https://doi.org/10.1016/j.ijrmhm.2019.04.011.

[35] C. Huber *et al.*, "3D Printing of Polymer-Bonded Rare-Earth Magnets With a Variable Magnetic Compound Fraction for a Predefined Stray Field," *Sci. Rep.*, vol. 7, no. 1, p. 9419, 2017, doi: 10.1038/s41598-017-09864-0.

[36] Z. Lu, O. I. Ayeni, X. Yang, H.-Y. Park, Y.-G. Jung, and J. Zhang, "Microstructure and Phase Analysis of 3D-Printed Components Using Bronze Metal Filament," *J. Mater. Eng. Perform.*, vol. 29, no. 3, pp. 1650–1656, 2020, doi: 10.1007/s11665-020-04697-x.

[37] C. Santos, D. Gatões, F. Cerejo, and M. T. Vieira, "Influence of Metallic Powder Characteristics on Extruded Feedstock Performance for Indirect Additive Manufacturing," *Materials*, vol. 14, no. 23. 2021. doi: 10.3390/ma14237136.

[38] L. Ren *et al.*, "Process Parameter Optimization of Extrusion-Based 3D Metal Printing Utilizing PW–LDPE–SA Binder System," *Materials*, vol. 10, no. 3. 2017. doi: 10.3390/ma10030305.

[39] L. Stepien, S. Gruber, M. Greifzu, M. Riede, and A. Roch, "Pure Copper: Advanced Additive Manufacturing," 2022.

[40] M. Mousapour, M. Salmi, L. Klemettinen, and J. Partanen, "Feasibility study of producing multi-metal parts by Fused Filament Fabrication (FFF) technique," *J. Manuf. Process.*, vol. 67, pp. 438–446, 2021, doi: https://doi.org/10.1016/j.jmapro.2021.05.021.

[41] S. H. Masood and W. Q. Song, "Thermal characteristics of a new metal/polymer material for FDM rapid prototyping process," *Assem. Autom.*, vol. 25, no. 4, pp. 309–315, Jan. 2005, doi: 10.1108/01445150510626451.

[42] Y. Zhang, L. Poli, E. Garratt, S. Foster, and A. Roch, "Utilizing

Fused Filament Fabrication for Printing Iron Cores for Electrical Devices," *3D Print. Addit. Manuf.*, vol. 7, no. 6, pp. 279–287, Dec. 2020, doi: 10.1089/3dp.2020.0136.

[43] M. F. Ernst, A. Maletzko, S. Baumann, N. Baumann, C. Hübner, and C.-C. Höhne, "FFF 3D Printing of Small Porous Structures from Polymer Compounds Using the Ultimaker 3," *Macromol. Mater. Eng.*, vol. 307, no. 10, p. 2200095, Oct. 2022, doi: https://doi.org/10.1002/mame.202200095.

[44] D. Nötzel, R. Eickhoff, C. Pfeifer, and T. Hanemann, "Printing of Zirconia Parts via Fused Filament Fabrication," *Materials*, vol. 14, no. 19. 2021. doi: 10.3390/ma14195467.

[45] R. Wick-Joliat, M. Schroffenegger, and D. Penner, "Multi-material ceramic material extrusion 3D printing with granulated injection molding feedstocks," *Ceram. Int.*, 2022, doi: https://doi.org/10.1016/j.ceramint.2022.10.170.

[46] V. Truxová, J. Šafka, J. Sobotka, J. Macháček, and M. Ackermann, "Alumina Manufactured by Fused Filament Fabrication: A Comprehensive Study of Mechanical Properties and Porosity," *Polymers*, vol. 14, no. 5. 2022. doi: 10.3390/polym14050991.

[47] T. Hanemann, D. Syperek, and D. Nötzel, "3D Printing of ABS Barium Ferrite Composites," *Materials*, vol. 13, no. 6. 2020. doi: 10.3390/ma13061481.

[48] C. Huber, S. Cano, I. Teliban, S. Schuschnigg, M. Groenefeld, and D. Suess, "Polymer-bonded anisotropic SrFe12O19 filaments for fused filament fabrication," *J. Appl. Phys.*, vol. 127, no. 6, p. 63904, 2020.

[49] E. Baudet, Y. Ledemi, P. Larochelle, S. Morency, and Y. Messaddeq, "3D-printing of arsenic sulfide chalcogenide glasses," *Opt. Mater. Express*, vol. 9, no. 5, pp. 2307–2317, 2019.

[50] I. Buj-Corral, D. Vidal, A. Tejo-Otero, J. A. Padilla, E. Xuriguera, and F. Fenollosa-Artés, "Characterization of 3D Printed Yttria-Stabilized Zirconia Parts for Use in Prostheses," *Nanomaterials*, vol. 11, no. 11. 2021. doi: 10.3390/nano11112942.

[51] D. Jiang and F. Ning, "Anisotropic deformation of 316L stainless steel overhang structures built by material extrusion based additive manufacturing," *Addit. Manuf.*, vol. 50, p. 102545, 2022.

[52] I. Buj, D. Vidal, A. Tejo, F. Fenollosa, J. El Mesbahi, and A. El Mesbahi, "Recent advances in the extrusion methods for ceramics," in *IOP Conference Series: Materials Science and Engineering*, 2021, vol. 1193, no. 1, p. 12030.

[53] P. Dudek, "FDM 3D printing technology in manufacturing composite elements," *Arch. Metall. Mater.*, vol. 58, no. 4, pp. 1415–1418, 2013.

[54] D. Zhang, X. Liu, and J. Qiu, "3D printing of glass by additive manufacturing techniques: A review," *Front. Optoelectron.*, vol. 14, no. 3, pp. 263–277, 2021.

[55] J. A. Slotwinski, E. J. Garboczi, P. E. Stutzman, C. F. Ferraris, S. S. Watson, and M. A. Peltz, "Characterization of metal powders used for additive manufacturing," *J. Res. Natl. Inst. Stand. Technol.*, vol. 119, p. 460, 2014.

[56] J. Chen and D. E. Smith, "Filament rheological characterization for fused filament fabrication additive manufacturing: A low-cost approach," *Addit. Manuf.*, vol. 47, p. 102208, 2021, doi: https://doi.org/10.1016/j.addma.2021.102208.

[57] C. Aumnate, S. Limpanart, N. Soatthiyanon, and S. Khunton, "PP/organoclay nanocomposites for fused filament fabrication (FFF) 3D printing," *Express Polym. Lett.*, vol. 13, no. 10, pp. 898–909, 2019.

[58] B. Arifvianto, Y. B. Wirawan, U. A. Salim, S. Suyitno, and M. Mahardika, "Effects of extruder temperatures and raster orientations on mechanical properties of the FFF-processed polylactic-acid (PLA) material," *Rapid Prototyp. J.*, 2021.

[59] H. Gonabadi, A. Yadav, and S. J. Bull, "The effect of processing parameters on the mechanical characteristics of PLA produced by a 3D FFF printer," *Int. J. Adv. Manuf. Technol.*, vol. 111, no. 3, pp. 695–709, 2020.

[60] M. J. Hooshmand, S. Mansour, and A. Dehghanian, "Optimization of build orientation in FFF using response surface methodology and posterior-based method," *Rapid Prototyp. J.*, vol. 27, no. 5, pp. 967–994, 2021.

[61] A. Boschetto, L. Bottini, F. Miani, and F. Veniali, "Roughness investigation of steel 316L parts fabricated by metal fused filament fabrication," *J. Manuf. Process.*, vol. 81, pp. 261–280, 2022.

[62] D. Godec, S. Cano, C. Holzer, and J. Gonzalez-Gutierrez, "Optimization of the 3D printing parameters for tensile properties of specimens produced by fused filament fabrication of 17-4PH stainless steel," *Materials (Basel).*, vol. 13, no. 3, p. 774, 2020.

[63] I. Ait-Mansour, N. Kretzschmar, S. Chekurov, M. Salmi, and J. Rech, "Design-dependent shrinkage compensation modeling and mechanical property targeting of metal FFF," *Prog. Addit. Manuf.*, vol. 5, no. 1, pp. 51–57, 2020.

[64] M. S. Tootooni, A. Dsouza, R. Donovan, P. K. Rao, Z. J. Kong, and P. Borgesen, "Classifying the Dimensional Variation in Additive Manufactured Parts from Laser-Scanned Three-Dimensional Point Cloud Data Using Machine Learning Approaches," *J. Manuf. Sci. Eng. Trans. ASME*, vol. 139, no. 9, pp. 1–14, 2017, doi: 10.1115/1.4036641.

[65] W. Tian, J. Ma, and M. Alizadeh, "Energy consumption optimization with geometric accuracy consideration for fused filament fabrication processes," *Int. J. Adv. Manuf. Technol.*, vol. 103, no. 5–8, pp. 3223–3233, 2019.

[66] R. Dastoorian, L. Wells, and W. Tian, "A Hybrid Approach for Heterogeneous High-Density Data for Surface Topology Classification: A Case Study," in *International Manufacturing Science and Engineering Conference*, 2019, vol. 58745, p. V001T02A019.

[67] Z. Ye, C. Liu, W. Tian, and C. Kan, "In-situ point cloud fusion for layer-wise monitoring of additive manufacturing," *J. Manuf. Syst.*, vol. 61, pp. 210–222, 2021.

[68] J. Gonzalez-Gutierrez, S. Cano, S. Schuschnigg, C. Kukla, J. Sapkota, and C. Holzer, "Additive manufacturing of metallic and ceramic components by the material extrusion of highly-filled polymers: A review and future perspectives," *Materials (Basel).*, vol. 11, no. 5, p. 840, 2018.

[69] L. M. Galantucci, A. Pellegrini, M. G. Guerra, and F. Lavecchia, "3D printing of parts using metal extrusion: an overview of shaping debinding and sintering technology," in *Proceedings of International Scientific Conference MMA*, 2021, pp. 5–12.

[70] M. Á. Caminero, A. Romero, J. M. Chacón, P. J. Núñez, E. García-Plaza, and G. P. Rodríguez, "Additive manufacturing of 316L stainless-steel structures using fused filament fabrication technology: Mechanical and geometric properties," *Rapid Prototyp. J.*, vol. 27, no. 3, pp. 583–591, 2021.

[71] J. González-Gutiérrez, G. B. Stringari, and I. Emri, "Powder injection molding of metal and ceramic parts," *Some Crit. Issues Inject. Molding*, pp. 65–88, 2012.

[72] P. Patel, T. R. Hull, R. W. McCabe, D. Flath, J. Grasmeder, and M. Percy, "Mechanism of thermal decomposition of poly(ether ether

ketone) (PEEK) from a review of decomposition studies," *Polym. Degrad. Stab.*, vol. 95, no. 5, pp. 709–718, 2010, doi: 10.1016/j.polymdegradstab.2010.01.024.

[73] H. Yang *et al.*, "Six-sigma quality management of additive manufacturing," *Proc. IEEE*, vol. 109, no. 4, pp. 347–376, 2020.

[74] P. K. Rao, J. Liu, D. Roberson, Z. Kong, and C. Williams, "Online Real-Time Quality Monitoring in Additive Manufacturing Processes Using Heterogeneous Sensors," *J. Manuf. Sci. Eng. Trans. ASME*, vol. 137, no. 6, pp. 1–12, 2015, doi: 10.1115/1.4029823.

[75] M. Moretti, F. Bianchi, and N. Senin, "Towards the development of a smart fused filament fabrication system using multi-sensor data fusion for in-process monitoring," *Rapid Prototyp. J.*, 2020.

[76] Z. Shi, A. Al Mamun, C. Kan, W. Tian, and C. Liu, "An LSTM-Autoencoder Based Online Side Channel Monitoring Approach for Cyber-Physical Attack Detection in Additive Manufacturing," *J. Intell. Manuf.*, 2021.

[77] E. Ferraris, J. Zhang, and B. Van Hooreweder, "Thermography based in-process monitoring of Fused Filament Fabrication of polymeric parts," *CIRP Ann.*, vol. 68, no. 1, pp. 213–216, 2019.

[78] M. Roy, R. Yavari, C. Zhou, O. Wodo, and P. Rao, "Prediction and experimental validation of part thermal history in the fused filament fabrication additive manufacturing process," *J. Manuf. Sci. Eng.*, vol. 141, no. 12, 2019.

[79] H. Wu, Y. Wang, and Z. Yu, "In situ monitoring of FDM machine condition via acoustic emission," *Int. J. Adv. Manuf. Technol.*, vol. 84, no. 5, pp. 1483–1495, 2016.

[80] J. Liu, Y. Hu, B. Wu, and Y. Wang, "An improved fault diagnosis approach for FDM process with acoustic emission," *J. Manuf. Process.*, vol. 35, pp. 570–579, 2018.

[81] T. Huang, S. Wang, S. Yang, and W. Dai, "Statistical process monitoring in a specified period for the image data of fused deposition modeling parts with consistent layers," *J. Intell. Manuf.*, vol. 32, no. 8, pp. 2181–2196, 2021.

[82] Z. Jin, Z. Zhang, and G. X. Gu, "Autonomous in-situ correction of fused deposition modeling printers using computer vision and deep learning," *Manuf. Lett.*, vol. 22, pp. 11–15, 2019, doi: 10.1016/j.mfglet.2019.09.005.

[83] A. Al Mamun, C. Liu, C. Kan, and W. Tian, "Securing Cyber-Physical Additive Manufacturing Systems by In-situ Process Authentication using Streamline Video Analysis," *J. Manuf. Syst.*, 2022.

[84] G. P. Greeff and M. Schilling, "Closed loop control of slippage during filament transport in molten material extrusion," *Addit. Manuf.*, vol. 14, pp. 31–38, 2017.

[85] Y. Chivel and I. Smurov, "On-line temperature monitoring in selective laser sintering/melting," *Phys. Procedia*, vol. 5, pp. 515–521, 2010.

[86] A. Lewis, M. Gardner, A. McElroy, T. Milner, S. Fish, and J. Beaman, "In-situ process monitoring and ex-situ part quality assessment of selective laser sintering using optical coherence tomography," in *2016 International Solid Freeform Fabrication Symposium*, 2016.

[87] M. Khanzadeh, W. Tian, A. Yadollahi, H. R. Doude, M. A. Tschopp, and L. Bian, "Dual process monitoring of metal-based additive manufacturing using tensor decomposition of thermal image streams," *Addit. Manuf.*, vol. 23, no. July, pp. 443–456, 2018, doi: 10.1016/j.addma.2018.08.014.

[88] M. Grasso, F. Gallina, and B. M. Colosimo, "Data fusion methods for statistical process monitoring and quality characterization in metal additive manufacturing," *Procedia CIRP*, vol. 75, pp. 103–107, 2018.

[89] C. Liu, Z. Kong, S. Babu, C. Joslin, and J. Ferguson, "An integrated manifold learning approach for high-dimensional data feature extractions and its applications to online process monitoring of additive manufacturing," *IISE Trans.*, vol. 53, no. 11, pp. 1215–1230, 2021.

[90] L. Kong, X. Peng, Y. Chen, P. Wang, and M. Xu, "Multi-sensor measurement and data fusion technology for manufacturing process monitoring: a literature review," *Int. J. Extrem. Manuf.*, vol. 2, no. 2, p. 22001, 2020.

[91] C. Liu, A. C. C. Law, D. Roberson, and Z. (James) Kong, "Image analysis-based closed loop quality control for additive manufacturing with fused filament fabrication," *J. Manuf. Syst.*, vol. 51, no. April, pp. 75–86, 2019, doi: 10.1016/j.jmsy.2019.04.002.

[92] J. Chung, B. Shen, and A. C. C. Law, "Reinforcement Learning-based Defect Mitigation for Quality Assurance of Additive Manufacturing," *arXiv Prepr. arXiv2210.17272*, 2022.

[93] J. Liu, C. Liu, Y. Bai, P. Rao, C. B. Williams, and Z. Kong, "Layer-wise spatial modeling of porosity in additive manufacturing," *IISE Trans.*, vol. 51, no. 2, pp. 109–123, 2019.

[94] S. H. Seifi, A. Yadollahi, W. Tian, H. Doude, V. H. Hammond, and L. Bian, "In Situ Nondestructive Fatigue-Life Prediction of Additive Manufactured Parts by Establishing a Process–Defect–Property Relationship," *Adv. Intell. Syst.*, p. 2000268, 2021.

[95] C. Liu *et al.*, "Toward Online Layer-wise Surface Morphology Measurement in Additive Manufacturing Using a Deep Learning-based Approach," *J. Intell. Manuf.*.

[96] Q. Tian, S. Guo, E. Melder, L. Bian, and W. Guo, "Deep Learning-based Data Fusion Method for In-Situ Porosity Detection in Laser-based Additive Manufacturing," *J. Manuf. Sci. Eng.*, vol. 143, no. April, pp. 1–38, 2020, doi: 10.1115/1.4048957.

[97] Z. Zhu, K. Ferreira, N. Anwer, L. Mathieu, K. Guo, and L. Qiao, "Convolutional Neural Network for geometric deviation prediction in Additive Manufacturing," *Procedia Cirp*, vol. 91, pp. 534–539, 2020.

[98] Q. Huang, H. Nouri, K. Xu, Y. Chen, S. Sosina, and T. Dasgupta, "Statistical predictive modeling and compensation of geometric deviations of three-dimensional printed products," *J. Manuf. Sci. Eng.*, vol. 136, no. 6, 2014.

[99] Q. Huang, "An analytical foundation for optimal compensation of three-dimensional shape deformation in additive manufacturing," *J. Manuf. Sci. Eng.*, vol. 138, no. 6, p. 61010, 2016.

[100] F. Ning, W. Cong, J. Qiu, J. Wei, and S. Wang, "Additive manufacturing of carbon fiber reinforced thermoplastic composites using fused deposition modeling," *Compos. Part B Eng.*, vol. 80, pp. 369–378, 2015, doi: https://doi.org/10.1016/j.compositesb.2015.06.013.

[101] H. L. Tekinalp *et al.*, "Highly oriented carbon fiber–polymer composites via additive manufacturing," *Compos. Sci. Technol.*, vol. 105, pp. 144–150, 2014, doi: https://doi.org/10.1016/j.compscitech.2014.10.009.

[102] W. Zhong, F. Li, Z. Zhang, L. Song, and Z. Li, "Short fiber reinforced composites for fused deposition modeling," *Mater. Sci. Eng. A*, vol. 301, no. 2, pp. 125–130, 2001, doi: https://doi.org/10.1016/S0921-5093(00)01810-4.

[103] A. S. Ramírez, R. D'Amato, F. B. Haro, M. I. Marcos, and J. M. de

Agustín del Burgo, “Composite material created by additive manufacturing techniques FFF and Robocasting for the manufacture of medical parts,” in *Proceedings of the Sixth International Conference on Technological Ecosystems for Enhancing Multiculturality*, 2018, pp. 410–415.

[104] C. Abeykoon, P. Sri-Amphorn, and A. Fernando, “Optimization of fused deposition modeling parameters for improved PLA and ABS 3D printed structures,” *Int. J. Light. Mater. Manuf.*, vol. 3, no. 3, pp. 284–297, 2020, doi: https://doi.org/10.1016/j.ijlmm.2020.03.003.

[105] A. Hamidi and Y. Tadesse, “Single step 3D printing of bioinspired structures via metal reinforced thermoplastic and highly stretchable elastomer,” *Compos. Struct.*, vol. 210, pp. 250–261, 2019, doi: https://doi.org/10.1016/j.compstruct.2018.11.019.

[106] S. Berretta, R. Davies, Y. T. Shyng, Y. Wang, and O. Ghita, “Fused Deposition Modelling of high temperature polymers: Exploring CNT PEEK composites,” *Polym. Test.*, vol. 63, pp. 251–262, 2017, doi: https://doi.org/10.1016/j.polymertesting.2017.08.024.